N O T I C E

THIS DOCUMENT HAS BEEN REPRODUCED FROM MICROFICHE. ALTHOUGH IT IS RECOGNIZED THAT CERTAIN PORTIONS ARE ILLEGIBLE, IT IS BEING RELEASED IN THE INTEREST OF MAKING AVAILABLE AS MUCH INFORMATION AS POSSIBLE

NASA Contractor Report 156869

Wallops Waveform Analysis of SEASAT-1 Radar Altimeter Data

Final Report

G. S. Hayne

July 1980

Wallops Flight Center
Wallops Island, Virginia 23337
AC 804   824-3411

NASA Contractor Report 156869

Wallops Waveform Analysis of SEASAT-1 Radar Altimeter Data

Final Report

G. S. Hayne

Applied Science Associates, Inc.
105 East Chatham St.
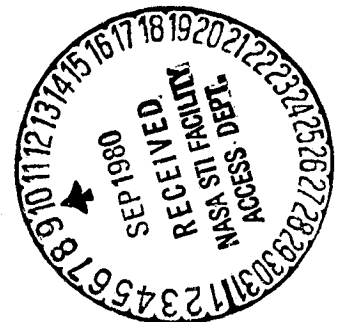Apex, NC 27502

NASA

National Aeronautics and
Space Administration .

Wallops Flight Center
Wallops Island, Virginia 23337
AC 804   824-3411

INTRODUCTION

This report describes the current status of work at Wallops Flight Center in the past year during which over-ocean data from the waveform samplers in the SEASAT-1 radar altimeter have been carefully analyzed in attempts to extract the skewness of the ocean surface elevation distribution. As described later, our work also provides information on possible tracking-point shifts due to changes in the surface distribution; a track-point shift is a type of altitude measurement error. The basic description of the radar altimeter is provided by Ref. 1, and Ref. 2 summarizes its performance evaluation. Preliminary results from our work had been contributed to the GOASEX-II Workshop in June 1979 (Ref. 3) and to a SEASAT Height/Orbit Accuracy Workshop in November 1979. Since then, we have spent considerable time trying to get around the difficulties of the combination of poor knowledge of the off-nadir attitude angle and the individual waveform samplers gain uncertainties, problems which will be described more fully later in this report.

There were several different motivations for this work. First, the problems we have encountered in the SEASAT-1 data analysis should be of immediate concern to the radar altimeters to be carried by the NOSS oceanographic satellite, and the data processing procedures we develop will carry over to the NOSS system. Second, one of the largest uncertainties in the SEASAT instrument height accuracy is the uncertainty in the possible track-point shift in response to changes in the ocean surface elevation distribution. Third, the surface skewness is a data product of considerable interest to oceanographers since, in combination with the significant waveheight (SWH), it allows estimating the ocean surface dominant wavelength based on the work of Huang and Long (Ref. 4). (See Ref. 3 or Ref. 5 for examples.) We are in the process of working on data from some of the

storms listed in the recent SEASAT Storms Workshop report (Ref. 6) and will report our results in a later publication.

The work reported here has been performed in collaboration with D. W. Hancock, III and with continuing help from E. J. Walsh. Additional assistance has been provided to us by R. G. Forsythe, J. Newell, and G. Quintana, and we have benefited from useful discussions with N. E. Huang, W. F. Townsend, C. L. Purdy, J. T. McGoogan, and J. L. MacArthur. The background for some of the waveform fitting lies in work performed during the research on SWH extraction in the GEOS-3 project under H. R. Stanley.

In the rest of this report we discuss the basic approach used, the waveform fitting procedure, and the model waveform fitted based on a near-Gaussian point-target response. The SEASAT-1 actual point-target response and its consequences are then discussed, followed by waveform sampler gains and attitude angle effects. Finally a brief summary section concludes the report.

BASIC APPROACH IN WALLOPS WAVEFORM ANALYSIS

The SEASAT-1 radar altimeter has a set of 63 waveform samplers which provide, once every tenth of a second, an average of the last 100 individual radar return waveforms. Sixty of these samplers are uniformly spaced, providing samples at every 3.125 nanoseconds along the radar return waveform, and the remaining three samplers are spaced 3.125 ns from each other and lie at the center of the set of 60 to increase the sampling density at the most important part of the return waveform (the "ramp" region). Table 1 lists the time location of these 63 samplers and establishes the numbering system for referring to them; we will refer to samplers 1 through 60 plus numbers $29\frac{1}{2}$, $30\frac{1}{2}$, and $31\frac{1}{2}$. In addition to the pre-launch data, two types of on-orbit calibration data are available for the 63 waveform samplers. In Calibration Mode I, the transmitted

TABLE 1. TIME LOCATION AND INDEXING FOR THE 63 SEASAT WAVEFORM SAMPLERS

Index	Time, ns	Previous SEASAT #	#, This Report	Index	Time, ns	Previous SEASAT #	#, This Report
1	-92.1875	-30	1	35	4.6875	+ 2	32
2	-89.0625	-29	2	36	7.8125	+ 3	33
3	-85.9375	-28	3	37	10.9375	+ 4	34
4	-82.8125	-27	4	38	14.0625	+ 5	35
5	-79.6875	-26	5	39	17.1875	+ 6	36
6	-76.5625	-25	6	40	20.3125	+ 7	37
7	-73.4375	-24	7	41	23.4375	+ 8	38
8	-70.3125	-23	8	42	26.5625	+ 9	39
9	-67.1875	-22	9	43	29.6875	+10	40
10	-64.0625	-21	10	44	32.8125	+11	41
11	-60.9375	-20	11	45	35.9375	+12	42
12	-57.8125	-19	12	46	39.0625	+13	43
13	-54.6875	-18	13	47	42.1875	+14	44
14	-51.5625	-17	14	48	45.3125	+15	45
15	-48.4375	-16	15	49	48.4375	+16	46
16	-45.3125	-15	16	50	51.5625	+17	47
17	-42.1875	-14	17	51	54.6875	+18	48
18	-39.0625	-13	18	52	57.8125	+19	49
19	-35.9375	-12	19	53	60.9375	+20	50
20	-32.8125	-11	20	54	64.0625	+21	51
21	-29.6875	-10	21	55	67.1875	+22	52
22	-26.5625	- 9	22	56	70.3125	+23	53
23	-23.4375	- 8	23	57	73.4375	+24	54
24	-20.3125	- 7	24	58	76.5625	+25	55
25	-17.1875	- 6	25	59	79.6875	+26	56
26	-14.0625	- 5	26	60	82.8125	+27	57
27	-10.9375	- 4	27	61	85.9375	+28	58
28	- 7.8125	- 3	28	62	89.0625	+29	59
29	- 4.6875	- 2	29	63	92.1875	+30	60
30	- 3.1250	- 1½	29½				
31	- 1.5625	- 1	30				
32	0.0000	0	30½				
33	1.5625	+ 1	31				
34	3.1250	+ 1½	31½				

radar pulse is fed directly to the sampler set through a variable attenuator; this provides the best available knowledge of the system point-target response function. In Calibration Mode II, a uniform signal is presented to the sampler set. Each sampler has a multiplicative gain differing slightly from its neighbors and Calibration Mode II is intended to provide the necessary gain correction information. Our work is based on the notion of using data from all 63 samplers, averaged over some suitable smoothing interval, and "best-fitting" these 63 experimental values to a model waveform by varying the model waveform's parameters until a minimum is reached in the sum of squares of the linefit residuals. Our usual smoothing interval is about 10 seconds, so that at SEASAT's rate of 1000 pulses per second, a waveform is fitted to a 10000 pulse estimate of the mean return.

The success or failure of this waveform-fitting will depend primarily upon the adequacy of the model waveform at representing the actual sampled waveform data being fitted, assuming that: i) the parameter-varying, the fitting itself, is performed adequately, and ii) that the correct gain calibrations are known and have been applied. Our work uses a model waveform described by seven parameters: i) amplitude; ii) time origin ("track-point"); iii) composite, or total, risetime; iv) baseline; v) composite, or total, skewness; vi) off-nadir attitude angle; and vii) composite, or total, kurtosis. In all work to date we have used a fixed zero kurtosis.

The six parameters fitted are necessary descriptors of the system-observed mean return waveform. The baseline for example is obviously present in the data and so must be fitted for, but is of little interest in itself. Listed below are several of the fitted parameters with comments in their possible uses or implications.

4

Amplitude - Not of much interest for now, but should be included in any attempts to refine the ocean surface reflectivity (σ°) measurements.

Attitude Angle - Of interest because of its use in estimating σ°. One can derive a theoretical σ° correction as a function of attitude. It was anticipation of the σ°-related need for good attitude estimates which led us originally to try to use all 63 waveform samplers in the fitting; more samples used from later in the waveform plateau should lead to more stable estimates of attitude.

Composite Risetime - This is used in the SWH estimation. The SEASAT-1 on-board processor produces estimates of SWH which are probably better than any user's current ability to use SWH; nonetheless, the six-parameter wave-form fitting will lead to a slightly different, somewhat more accurate SWH value than the on-board processor.

Composite Skewness - This contains the ocean surface skewness, an oceano-graphic parameter of considerable potential interest. We do not yet know the limiting stability of the ocean surface skewness estimated from the SEASAT-1 experimental data but will be determining the skewness stability in our continuing waveform analysis research.

Time Origin - This parameter indicates the fitted waveform position rela-tive to the set of waveform samplers, and hence can be used to provide a correction to the altimeter's altitude output. The waveform fitting pro-cedure can be viewed as providing a "software tracker" which replaces, after the fact, the results from the SEASAT-1 hardware tracker. Possible shifts in the hardware tracking point due to changes in the ocean surface's distribution will show up as changes in the time-origin parameter.

WAVEFORM FITTING ROUTINE

The model waveform to be fitted is supplied as a subroutine to the overall fitting procedure. The entire fitting routine is quite general and permits: i) varying the number of experimental data points being fitted; ii) varying the number and order of the waveform parameters being fitted; iii) applying constraints to one or more of the fitted parameters; and iv) uniform or non-uniform weighting of the input data. In the work to date, the experimental data have been uniformly weighted. We have found that the solutions seem more stable if the skewness and the pointing angle are slightly constrained when they are among the fitted parameters. The overall fitting routine is a straightforward generalization and extension of the approach sketched in Ref. 7 for a four-parameter situation. A description of the general fitting program will be published as a separate report, but a Fortran source listing and further comments may be obtained in the meantime by contacting either G. S. Hayne or D. W. Hancock, III at NASA Wallops Flight Center.

MODEL WAVEFORM FITTED

Based on earlier work of a number of researchers as summarized in Ref. 8, it is assumed that the correct mean return waveform from a typical radar altimeter can be obtained from the convolution of the following three terms: i) the average impulse response function of the quasi-calm ocean surface (the "flat sea"), ii) the ocean surface elevation distribution function for the "effective radar scattering elements," and iii) the radar system point-target response function. The first of these terms, the quasi-calm ocean impulse response function, is provided by Ref. 8. It looks somewhat like a unit step function with a subsequent "plateau" behavior which is a function of the antenna beam-

6

width and off-nadir angle. Figure 1 shows the flat-sea impulse response functions for several different off-nadir angles for SEASAT-1 and for GEOS-3. The location of the "altitude gate," a wide waveform sampling gate, is shown for later discussion. Note that the Figure 1 response functions have been renormalized to include (approximately) the effects of the SEASAT-1 and GEOS-3 AGC systems. In this report we are concerned with the shape of the impulse response functions and the waveforms, not the amplitude as such. The surface reflectivity, σ^0, is treated in the rest of this report as an arbitrary unknown multiplier; its value can be estimated through analysis of the AGC signal, but this report will not treat the σ^0 estimation further.

The second term in the convolution is the radar-observed surface elevation probability density function (pdf) and in past work it has been assumed that the radar-observed elevation pdf is the same as the true, geometrical surface elevation pdf. I have discussed this briefly in Ref. 9. Ref. 10 is a recent paper which treats the differences in distribution on a theoretical basis, but for the work in this report it is sufficient to assume that there is some distribution varying with SWH and to put off these more serious questions of what distribution until later.

The third term in the convolution, the system point-target response, is the radar altimeter's transmitted pulse shape as sampled at the receiver by the 63 waveform samplers in the SEASAT instrument. We use the phrase "system point-target response" here instead of the more casually used "radar pulse shape" because what is meant is the transmitted radar pulse as modified by receiver effects. The reader might for ease of physical interpretation prefer to think of the point-target response as the same as the transmitted pulse, and this is nearly correct.

Figure 1. Calm sea impulse response functions vs time for GEOS-3 and SEASAT-1 radar altimeters. (These functions are zero for all times less than zero.)
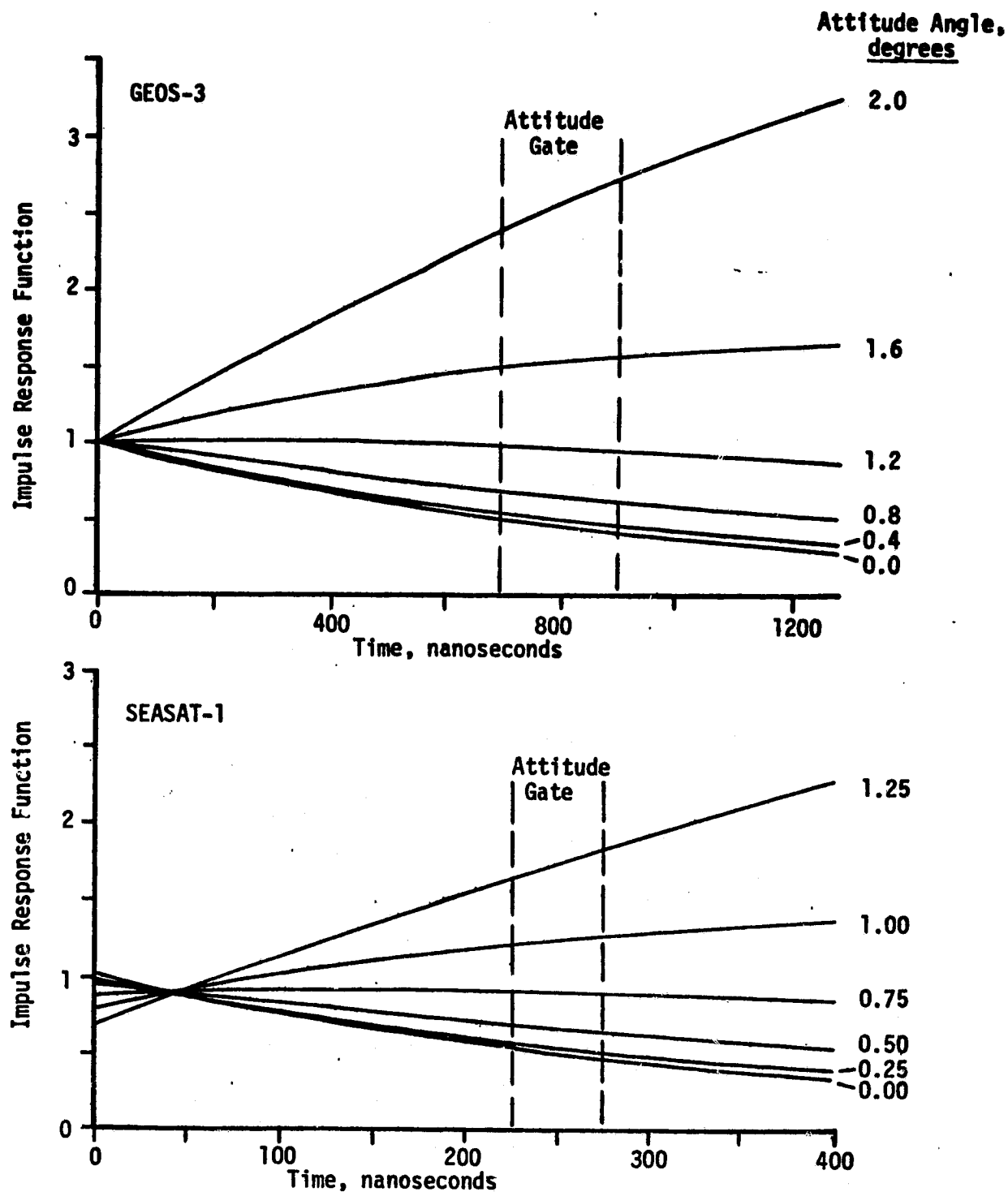
The convolution of the three terms just described is shown schematically in Figure 2 in which $P_{FS}(t)$ is the function already shown in Figure 1. Notice that all three terms in the convolution are assumed to be time functions. The surface elevation pdf is a spatial distribution but can be transformed to a time function by using the altimeter's (two-way) ranging velocity of light, $c/2 = 0.15$ meters per nanosecond. In Figure 2, both the surface elevation pdf, $q_s(t)$ and the radar system point-target response, $s_r(t)$, are sketched as being nearly Gaussian. In this report we will refer to a function's being nearly Gaussian as meaning specifically that the function, $q_s(t)$ for example, can be adequately represented by the skewed Gaussian form

$$q_s(t) = \left[1 + (t^3/\sigma_s^3 - 3t/\sigma_s)\lambda_s/6 \right] \frac{1}{\sqrt{2\pi}\ \sigma_s} \exp\left[-\frac{1}{2}(t/\sigma_s)^2 \right] ,$$
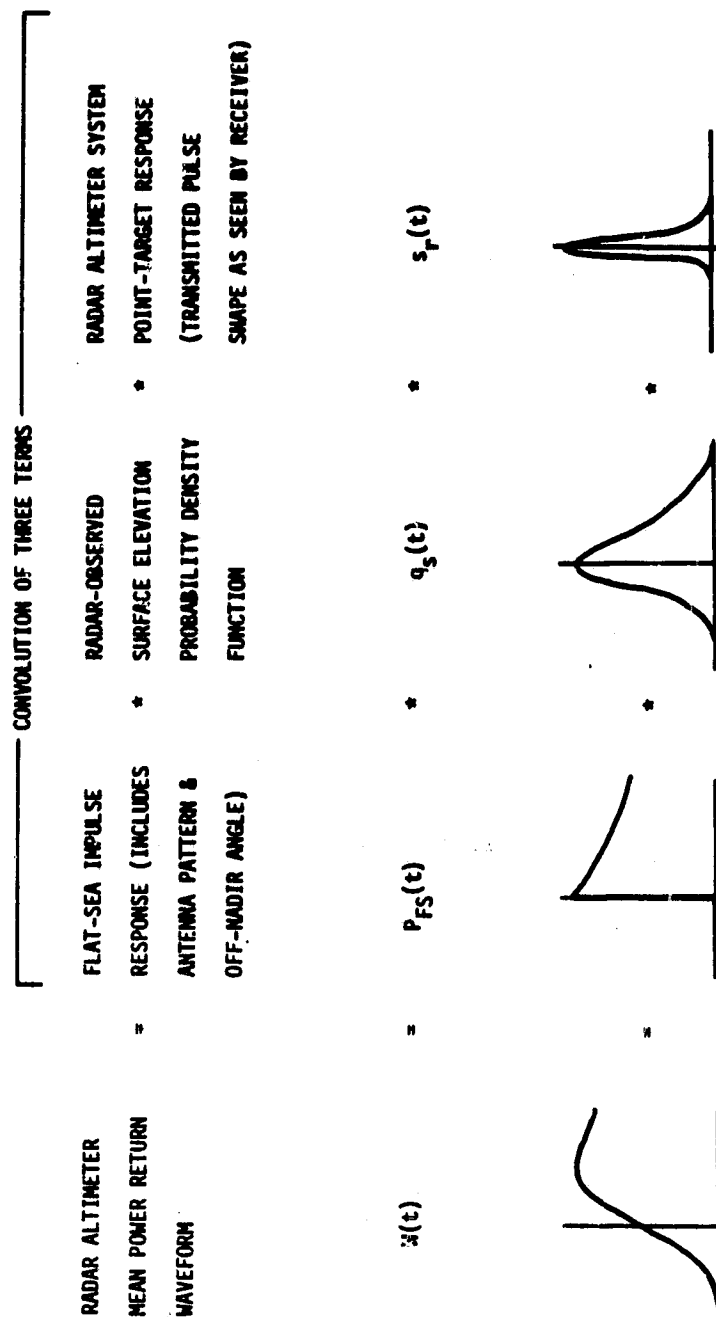
where σ_s is the second moment (the "width") and λ_s is the skewness. The skewness is dimensionless and σ_s has time units, nanoseconds in this work. If the system point-target response function $s_r(t)$ is also nearly Gaussian with width σ_r and skewness λ_r, then the convolution $s_r(t) * q_s(t)$ will also have this same nearly Gaussian form (neglecting higher moments) with a composite width σ_c and composite skewness λ_c given by

$$\sigma_c = [\sigma_s^2 + \sigma_r^2]^{\frac{1}{2}}$$

and

$$\lambda_c = (\sigma_s/\sigma_c)^3 \lambda_s + (\sigma_r/\sigma_c)^3 \lambda_r .$$

Figure 2. Mean return waveform from convolution.

CONVOLUTION OF THREE TERMS

| RADAR ALTIMETER MEAN POWER RETURN WAVEFORM | = | FLAT-SEA IMPULSE RESPONSE (INCLUDES ANTENNA PATTERN & OFF-NADIR ANGLE) | * | RADAR-OBSERVED SURFACE ELEVATION PROBABILITY DENSITY FUNCTION | * | RADAR ALTIMETER SYSTEM POINT-TARGET RESPONSE (TRANSMITTED PULSE SHAPE AS SEEN BY RECEIVER) |

$\overline{P}(t)$ = $P_{FS}(t)$ * $q_s(t)$ * $s_r(t)$

A separate paper (Ref. 9, also Ref. 10) gives a several-term series expansion which for SEASAT-1 adequately approximates the convolution of a nearly Gaussian form with the $P_{FS}(t)$ of Figure 1. The advantage of the results in Ref. 9 is that the two convolutions indicated in Figure 2 can be replaced by expressions whose evaluation requires much less computer time than would numerical convolutions.

Figures 3 and 4 are reprinted from Ref. 10 and show the dependence of the mean return waveform on SWH and on attitude angle for a radar altimeter having a pure Gaussian point-target response function with the SEASAT-1 nominal design pulsewidth, and with the SEASAT-1 antenna beamwidth and satellite altitude. Figure 5, also reprinted from Ref. 10, shows the difference that a surface skewness will make in the radar altimeter's mean return waveform. A skewness magnitude of 0.5 is about the outside limit that anyone might expect for a real ocean surface elevation distribution, so Figure 5 shows the outside limits for the skewness-caused waveform changes in the SEASAT case and shows something of the difficulty of any attempts to measure a surface skewness.

All of the Wallops waveform work is based on the waveform expansion given in Ref. 9. In the event that the radar system point target response function cannot be adequately represented by a nearly Gaussian function, we still use the expressions given in Ref. 9 to represent the convolution of the flat-sea impulse response with the surface elevation pdf (convolution of $P_{FS}(t)$ and $q_s(t)$ in Figure 2); a numerical convolution of this result with the point target response ($s_r(t)$ in Figure 2) then gives the complete waveform. In other words, we use the Ref. 9 expressions to represent "everything else," everything but the point target response function, and then convolve the "everything else" function with the point-target response for the complete waveform. With the Ref. 9 waveform as the starting point for the Wallops work, the difficulties encoun-

11

Figure 3. SEASAT-1 mean return waveform change with significant waveheight.

$\xi=0.0$

$A=100, \quad \sigma_r=1.327$ ns

$t_0=\lambda_r=\kappa_r=\lambda_s=\kappa_s=0.$

4-Term Expansion

Significant Wave-
height, Meters

18
15
12
9
6
3
0

TIME, NANOSECONDS

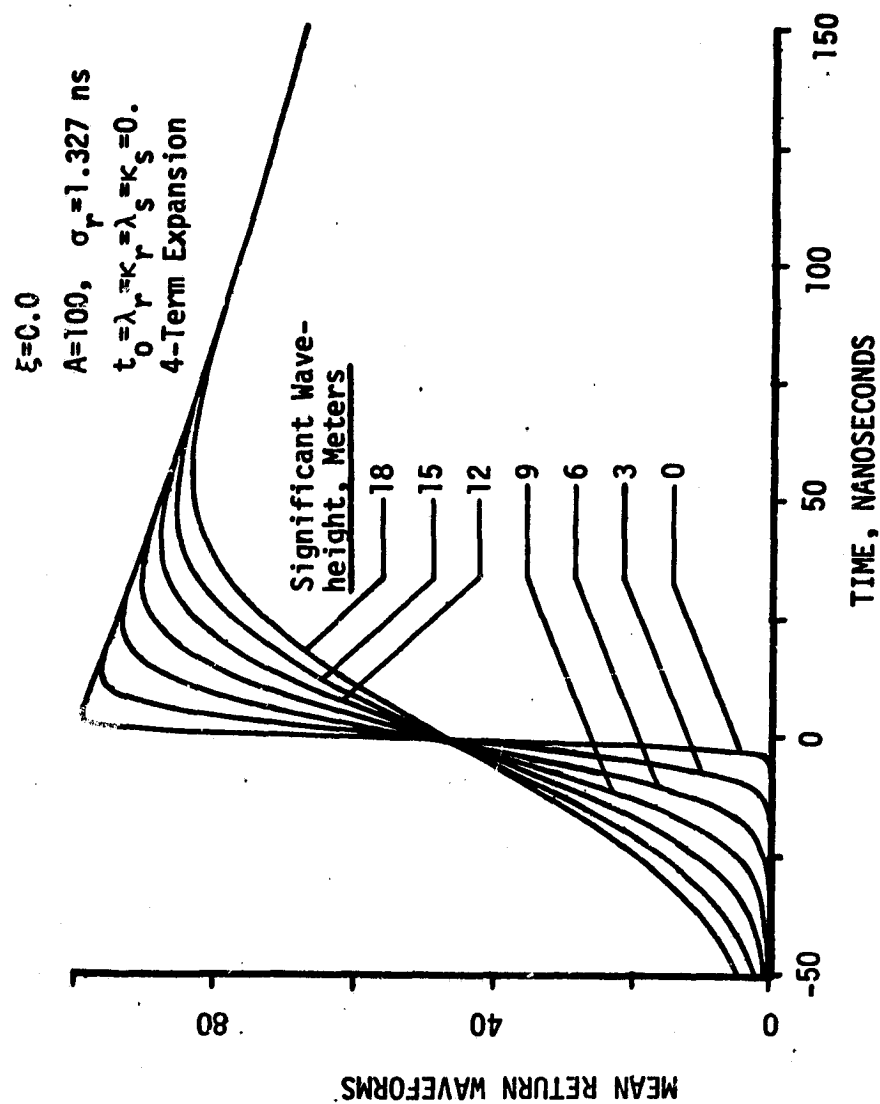MEAN RETURN WAVEFORMS

80

40

0

-50   0   50   100   150

Figure 4.   SEASAT-1 mean return waveform change with off-nadir angle.
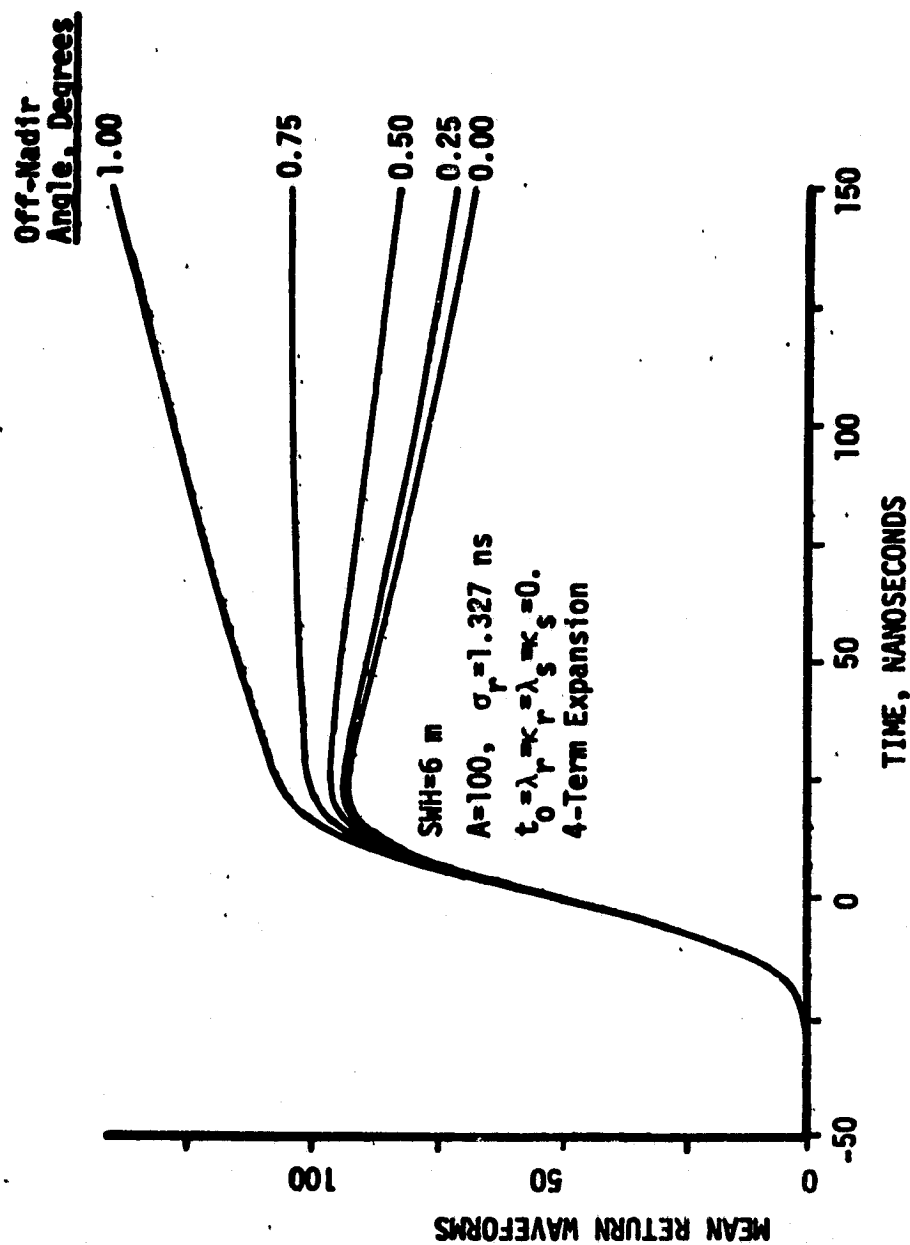
**Figure 5. SEASAT-1 mean return waveform change with skewness.**

SWH=6 m, ξ=0.0°
A=100, σ_r=1.327 ns
t_o=λ_r=κ_r=κ_s=0.
4-Term Expansion

$W(\lambda_s=0)$

$W(\lambda_s=-0.5)$

$10\times[W(\lambda_s=0)-W(\lambda_s=-0.5)]$

TIME, NANOSECONDS

MEAN RETURN WAVEFORMS & DIFFERENCES

SEASAT Waveform Sampling Gates

14
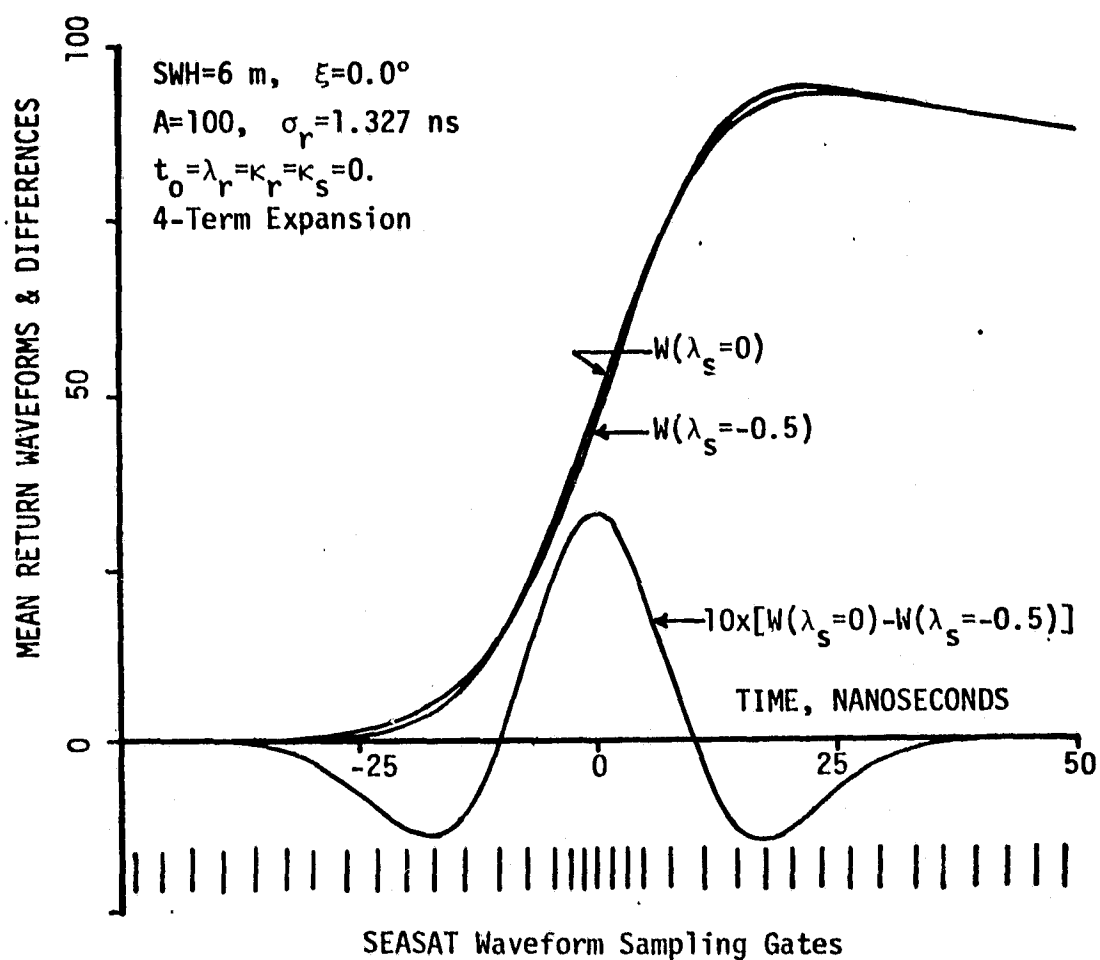
tered included i) the actual shape of the point-target response, ii) individual sampler gain biases, and iii) knowledge of the off-nadir attitude angle. These items will be described in following sections of this report. The terms "off-nadir angle," "attitude angle," or "attitude" are treated as interchangeably synonymous with each other and with "altimeter pointing angle off-nadir" in the following discussions.

ACTUAL SEASAT-1 POINT-TARGET RESPONSE AND ITS CONSEQUENCES

The SEASAT-1 nominal design system point-target response was 3.125 nanoseconds wide at 1/2-power points, and the on-board processor for SWH was designed assuming this to be a Gaussian shape with a second moment value 1.327 ns (the ratio of the half-power full-width to the second moment of a Gaussian function is 2.355; 3.125 ns ÷ 2.355 = 1.327 ns). The unweighted chirp transmitted radar pulse is supposed to have a $[(\sin x)/x]^2$ form, and a first-order correction to the SWH to account for the non-Gaussian shape is described in Ref. 1. This correction was simply to replace the 3.125 ns pulse by a Gaussian function 20% wider in the SWH calculation, and the SEASAT data processing at JPL includes a look-up table which makes this correction. Figure 6 shows the actual system point-target response averaged from eight sets of Calibration Mode I, Step 9 data from the SEASAT-1 waveform samplers. The only half-integer-numbered waveform samplers are numbers 29½, 30½, and 31½ (see Table 1 for notation), and in Figure 6 we have put zero values (except for the noise baseline) at every other half-integer location (where nulls should have occurred in the (sin x)/x pulse). This figure, assuming the individual sampler gains are correct, represents the best available knowledge of the actual system point-target response function. Because the point-target response in Figure 6 is obviously not

15

Figure 6. SEASAT Radar Altimeter System Point-Target Response
from CAL Step 9 after Gain Bias Corrections
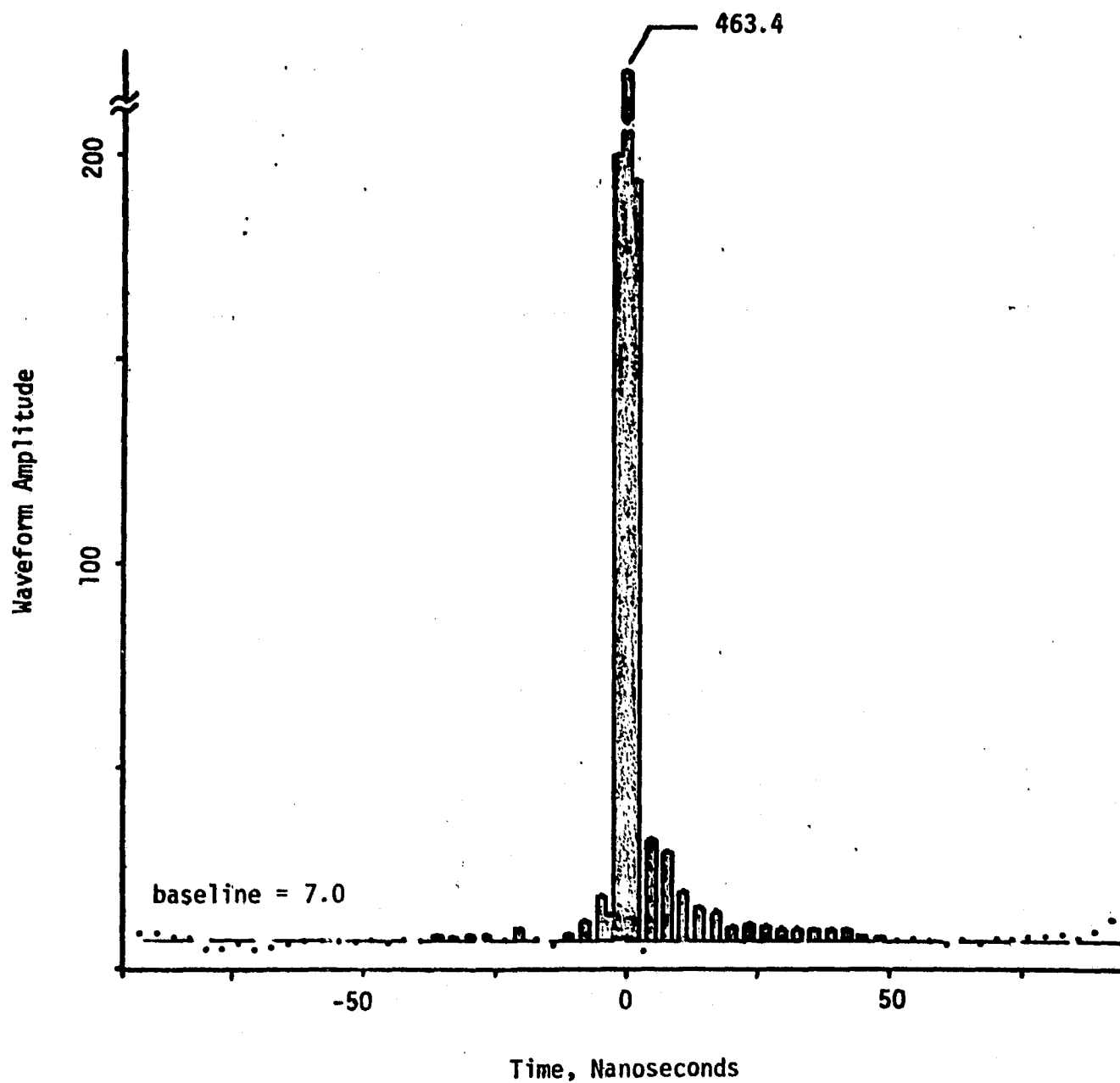
Gaussian, not $[(\sin x)/x]^2$, not even symmetric, a waveform fitting procedure based on a near-Gaussian point-target response will be fitting the data to the wrong model waveform with the consequence that every fitted parameter will be in error. These errors decrease as SWH increases (as the surface distribution's second moment becomes appreciably larger than the second moment of the point-target response). Figures 7 and 8 show the results of fitting the Gaussian-based model waveform of Ref. 9 to the mean return waveform samples which would be the result of a near-Gaussian surface distribution and the system point-target response shown in Figure 6. The "data," the individual points in Figures 7 and 8, are generated by a numerical convolution of the point-target response of Figure 6 with an "everything else" function from Ref. 9, and the solid lines in Figures 7 and 8 are the fitted waveforms using the incorrect model waveform (that is, the Ref. 9 results based on a near-Gaussian point-target response). Every parameter fitted has some degree of error, and this is particularly extreme in Figure 7 for zero input SWH; the incorrect solution gives an off-nadir angle of nearly 0.4° although the true input angle was 0.0°.

The true point-target response of Figure 6 can be built into the line-fitting procedure by incorporating within the model waveform subroutine a numerical convolution of the point-target response and the "everything else" functions; the penalty for this is considerably longer computation times in the waveform analysis programs. Our waveform analysis programs were written for research purposes with a high degree of flexibility and for ease of model function modification and no particular effort has been directed at writing efficient source code for reducing computation times, but some idea of the time-penalty of the numerical convolution within the model waveform can be gotten from our program's running times on a medium-sized digital computer. A six-parameter fit of the near-Gaussian point-target response function model waveform

Figure 7. Waveform based on near-Gaussian point target
response but fitted to model data based on
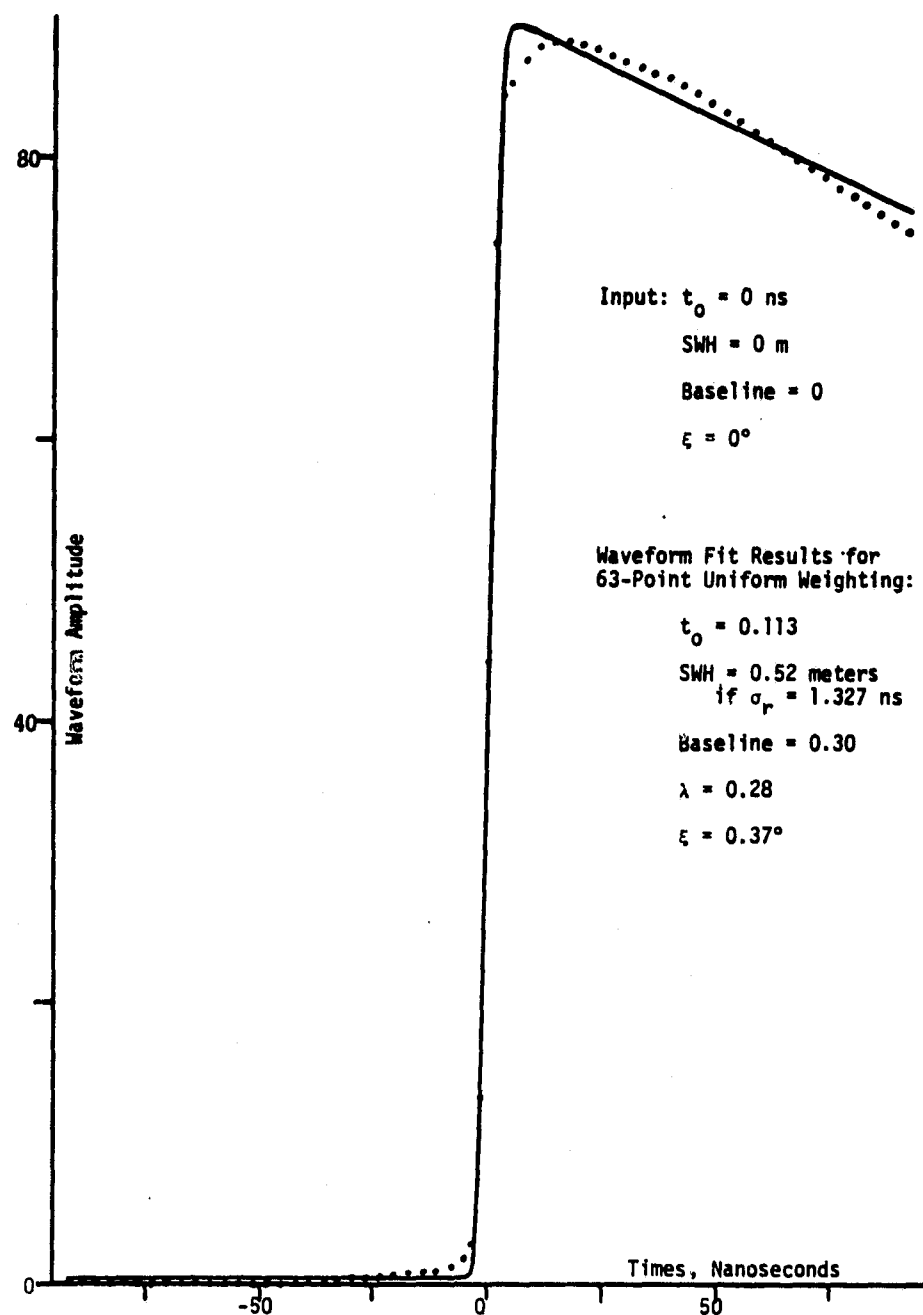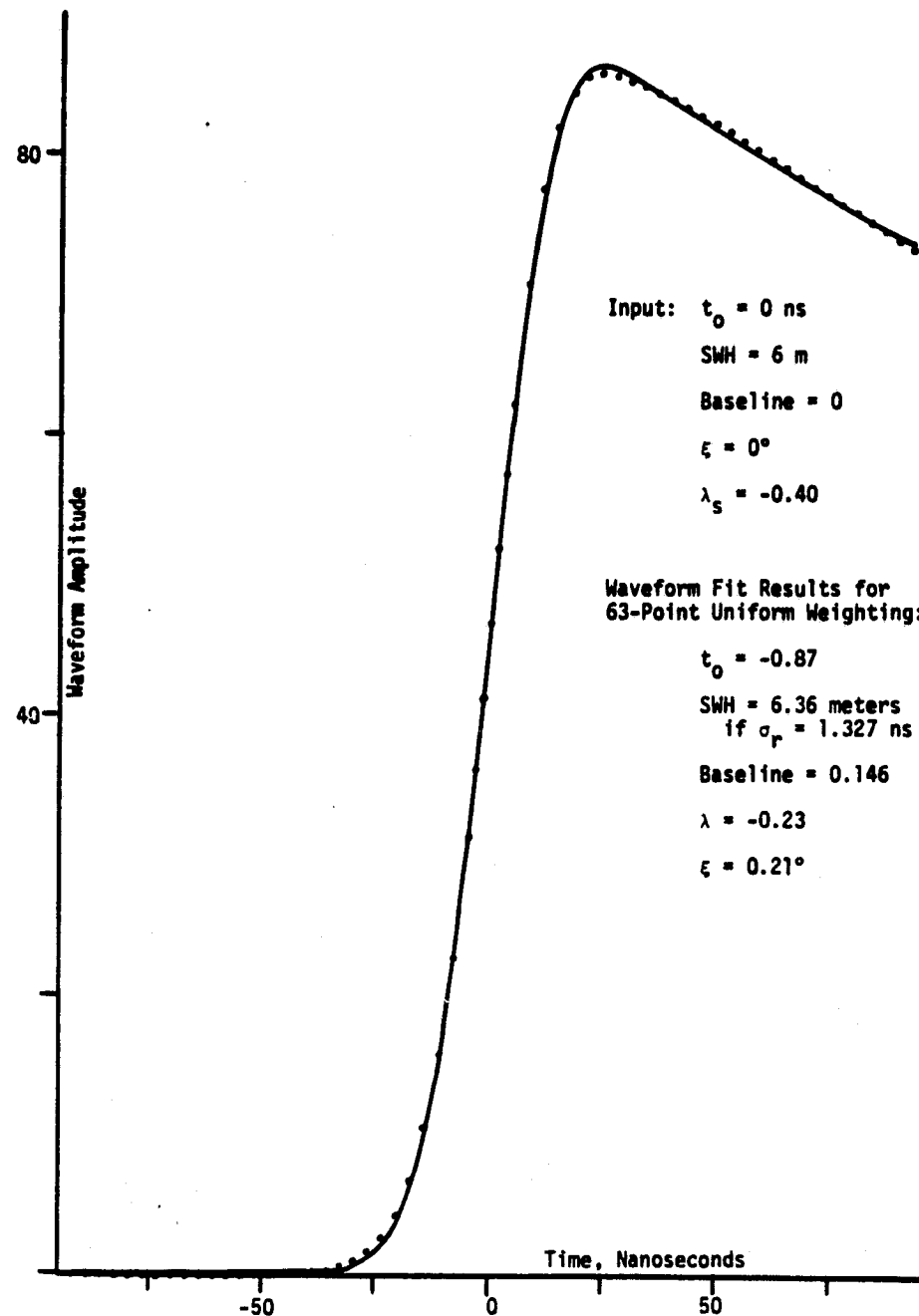actual SEASAT-1 point target response of
Figure 6.

Input: t_o = 0 ns

SWH = 0 m

Baseline = 0

ξ = 0°

Waveform Fit Results for
63-Point Uniform Weighting:

t_o = 0.113

SWH = 0.52 meters
  if σ_r = 1.327 ns

Baseline = 0.30

λ = 0.28

ξ = 0.37°

Figure 8. Waveform based on near-Gaussian point target response but fitted to model data based on actual SEASAT-1 point target response of Figure 6.

Input: $t_o = 0$ ns

SWH = 6 m

Baseline = 0

$\xi = 0°$

$\lambda_s = -0.40$

Waveform Fit Results for
63-Point Uniform Weighting:

$t_o = -0.87$

SWH = 6.36 meters
if $\sigma_r = 1.327$ ns

Baseline = 0.146

$\lambda = -0.23$

$\xi = 0.21°$

(represented solely by the expressions of Ref. 9) to 63 waveform samples ran in somewhat less than one second. In contrast, the "correct model" incorporating numerical convolution with the point target response of Figure 6 required 30 seconds or more to fit the same data.

This discussion has been concerned with two different considerations: i) adequacy of representing the actual expected mean waveform, and ii) computer running time. We indicated two different approaches which, in the rest of this report, will be referred to as i) the "incorrect but fast" model waveform, and ii) the "correct but slow" model waveform. The "incorrect but fast" waveform assumes the point-target response to be Gaussian and then uses the general expressions of Ref. 9 to give the waveform directly. The "correct but slow" waveform uses the Ref. 9 expressions as the "everything else" function which is then numerically convolved with the actual point-target response of Figure 6 to give the final waveform.

CORRECTION CURVES ALLOWING USE OF "INCORRECT BUT FAST" MODEL WAVEFORM

This paragraph will describe one possible way to avoid paying the penalty of longer computation times and still take account of the effects of the real system point-target response function. It should be possible to use the "incorrect but fast" waveform model (as defined in the last paragraph above) in the waveform fitting and then correct the resulting fitted parameters by using a separately-generated correction table. This possibility is suggested by Figures 7 and 8 on which the correct (input) parameters and the incorrect (fitted) values are listed; for the particular cases in these figures we have the necessary correction data. A simulation program has been written here which produces the correct waveform incorporating the sampled point-target response effects and

fits the "incorrect but fast" model waveform to these points. By varying the input parameter values systematically and comparing the results, the desired correction curves can be obtained. Figures 9 through 12 show the needed correction curves for SWH, time origin ("track point"), off-nadir attitude, and surface skewness, respectively, for 63-point, six-parameter, uniformly-weighted data fitting with the skewness and attitude angle lightly constrained. Any change in these conditions, number of points or parameters fitted and so forth, would necessitate rerunning the entire simulation to generate a new set of correction curves for the new conditions. There is nothing in the generation of the correction curves to account for errors in individual waveform sampler gains; that possible problem must already have been solved. A built-in assumption in generating Figures 9 through 12 was that for a given set of input parameters, the average of a number of waveform fits from waveform samples with typical random noise would converge to the zero-noise result. Figures 9 through 12 were generated for zero-noise waveform samples, equivalent to infinite averaging time, but for the ten second, 1000 pulse averages of actual SEASAT-1 data that we have been using the noise standard deviation is around 3% of the mean level in each sampler. We have since added realistic random noise to the simulation program and the mean values of the fitted parameters from the noisy simulated data do seem to converge to the results of the zero-noise case but this conclusion is based on a limited number of runs and more work is needed on this question.

Figure 9. SEASAT-1 SWH corrections.

True Surface
Skewness (Time)

-0.6
-0.4
-0.2
0.0

Fitted ("incorrect but fast") Significant Waveheight, Meters

Additive Significant Waveheight Correction, Meters
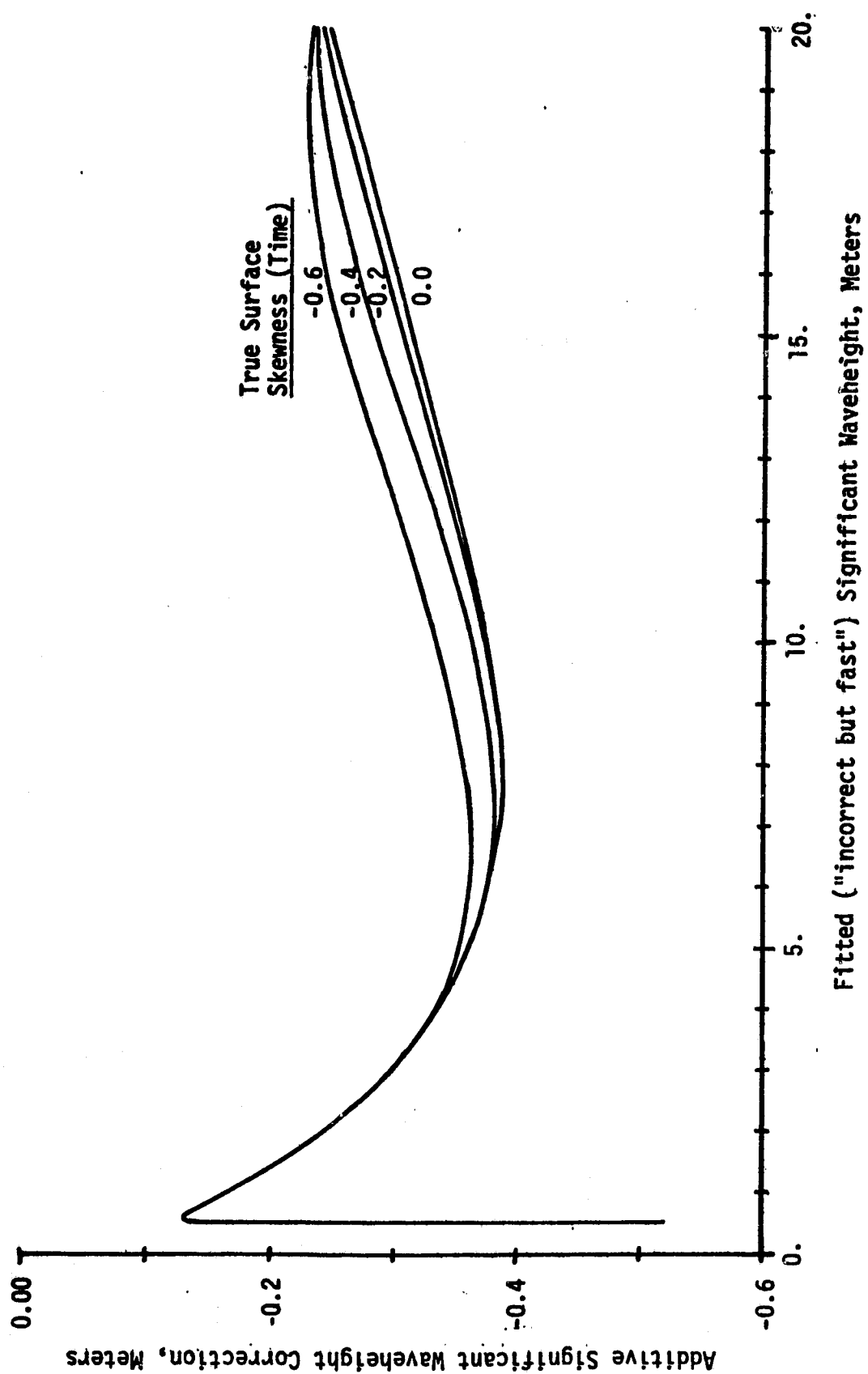
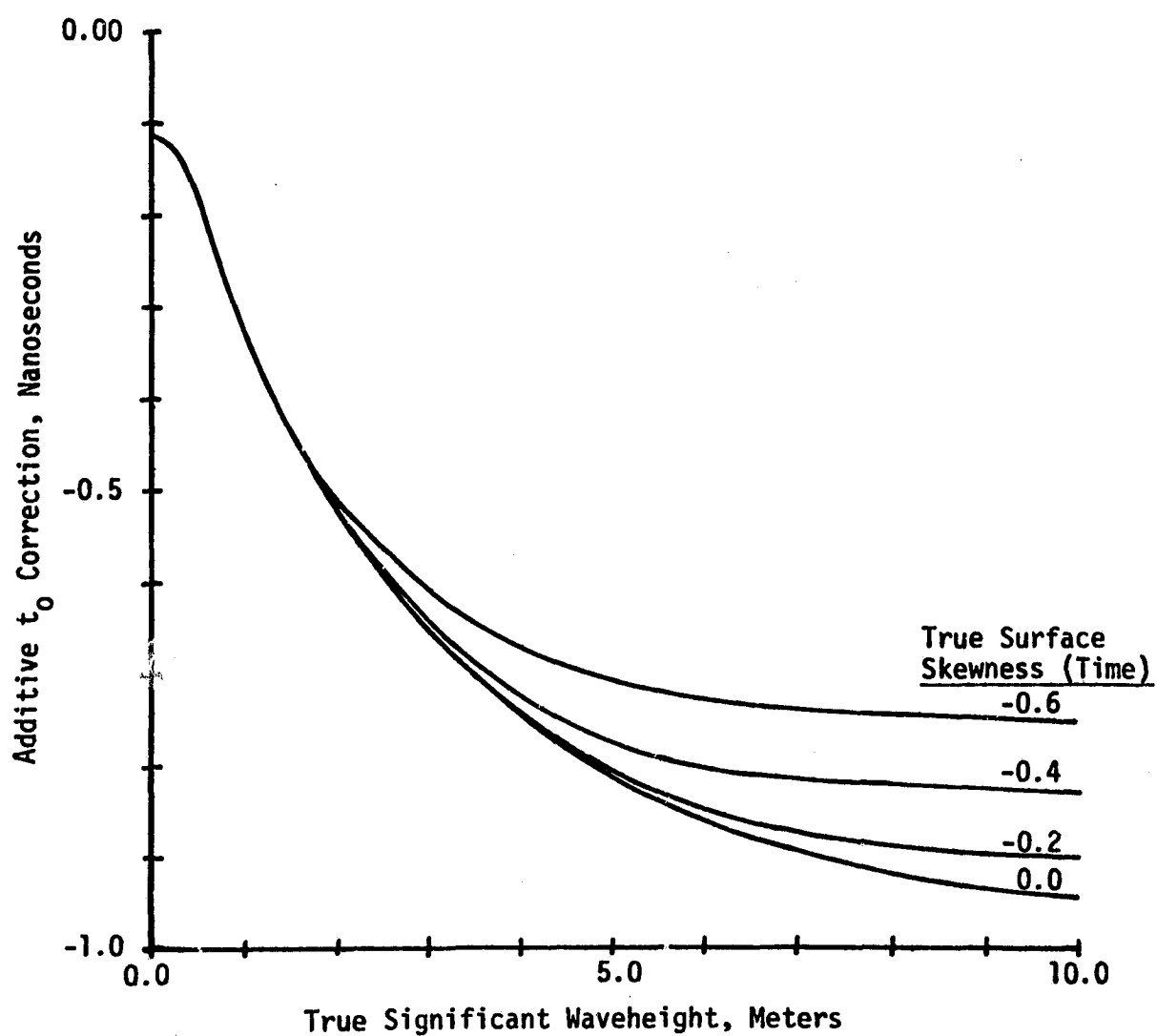Figure 10.   SEASAT-1 time origin corrections.
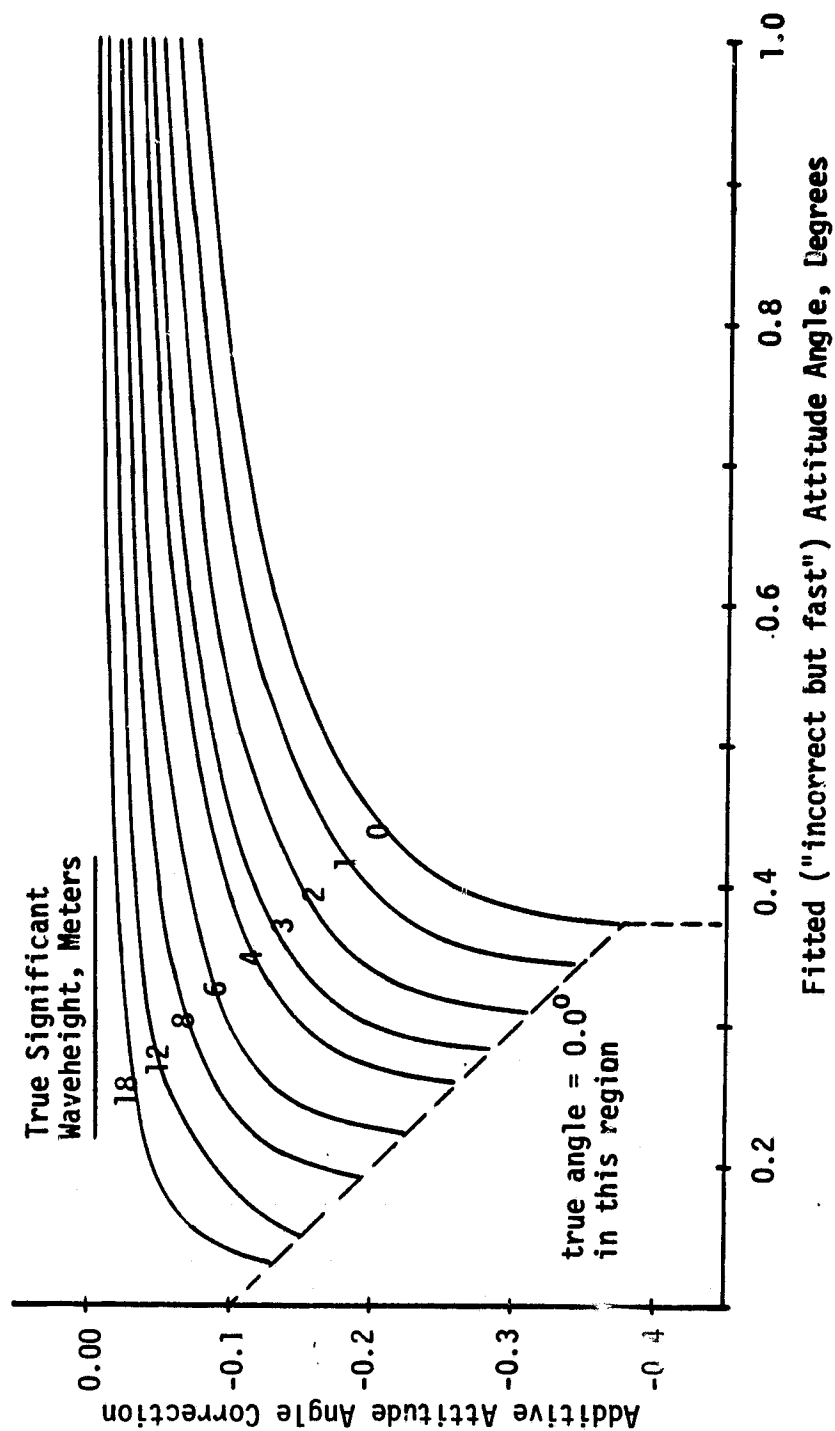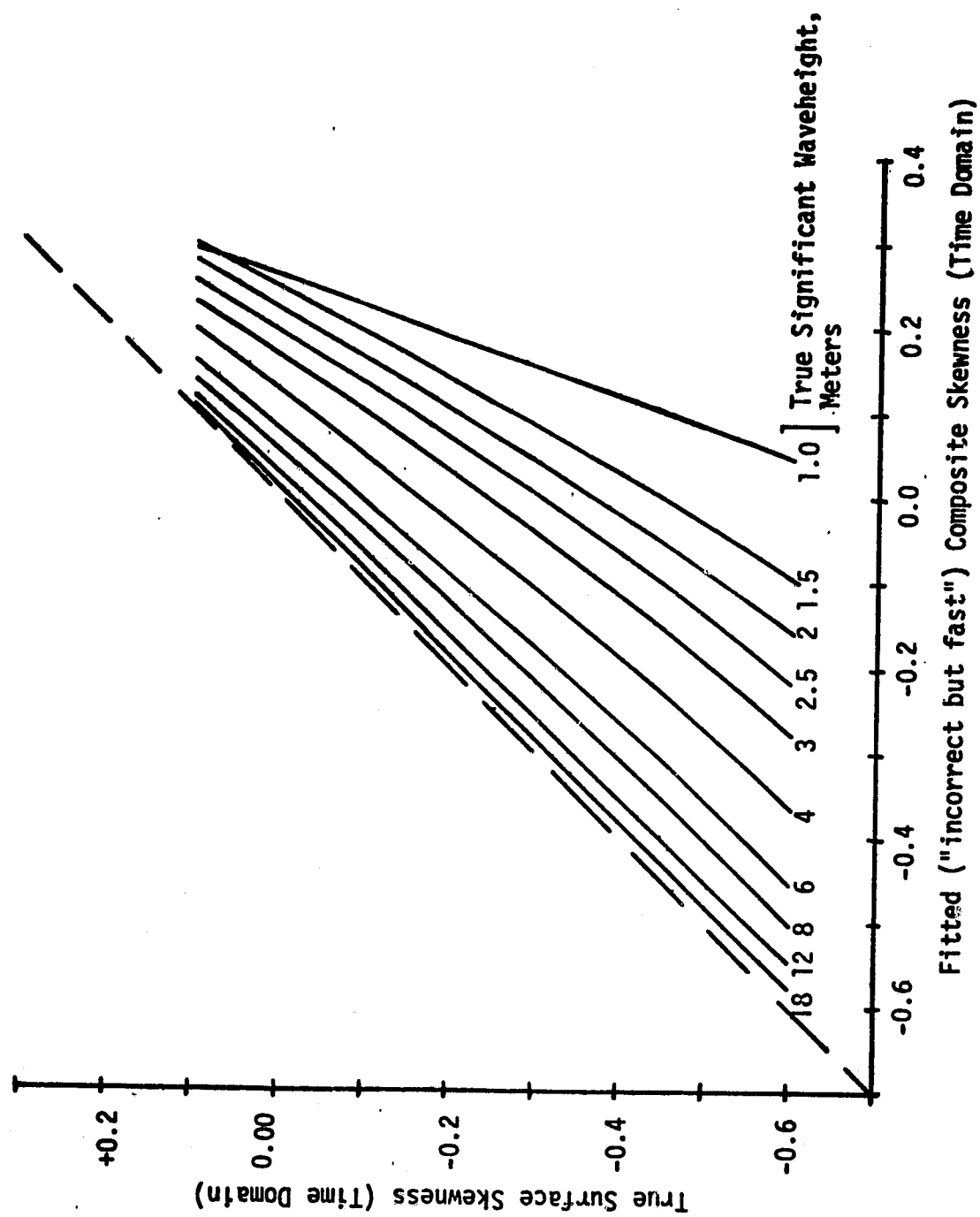
Figure 11. SEASAT-1 attitude corrections.

Figure 12. SEASAT-1 skewness corrections.

WAVEFORM SAMPLER GAIN ADJUSTMENTS

Preliminary results from our first waveform fitting to the SEASAT-1 data indicated that there were individual sampling data biases and that some method had to be developed for "fine-tuning" the individual sampler gains after using the Calibration Mode II data as a starting point for these gains. Obvious patterns were visible in the residuals after the waveform fitting; some of the sampler's residuals appeared always to be positive, others negative, and we intended using averages of these residuals over a number of sets of input data to fine-tune the starting gains. This situation is similar to the earlier GEOS-3 radar altimeter, although there additive gain biases were assumed rather than the present cases' multiplicative gain biases because of the hardware differences. Walsh, for example, described a GEOS-3 sampler bias adjustment procedure in Ref. 5.

Figure 13 is a summary of the gain bias fine-tuning which we initially intended using. This procedure was in fact used in our data reduction just prior to the GOASEX II Workshop in June 1979 and in the Wallops contribution to the altimeter portion of the report from the workshop (Ref. 3). An implicit assumption for the process in Figure 13 is that the gain bias adjustments needed are relatively small and that the individual sampler final gains are distributed more or less randomly around the starting-point gains from Calibration Mode II. There is also the requirement that the off-nadir angle be known, and for the early June 1979 work we used the SEASAT attitude control system-derived angle as available from the JPL-processed data tapes. Figure 13 indicates an optional final adjustment over the full sampler set, but we have not used that option in work to date.

Figure 13. Summary of gain fine-tuning procedure.
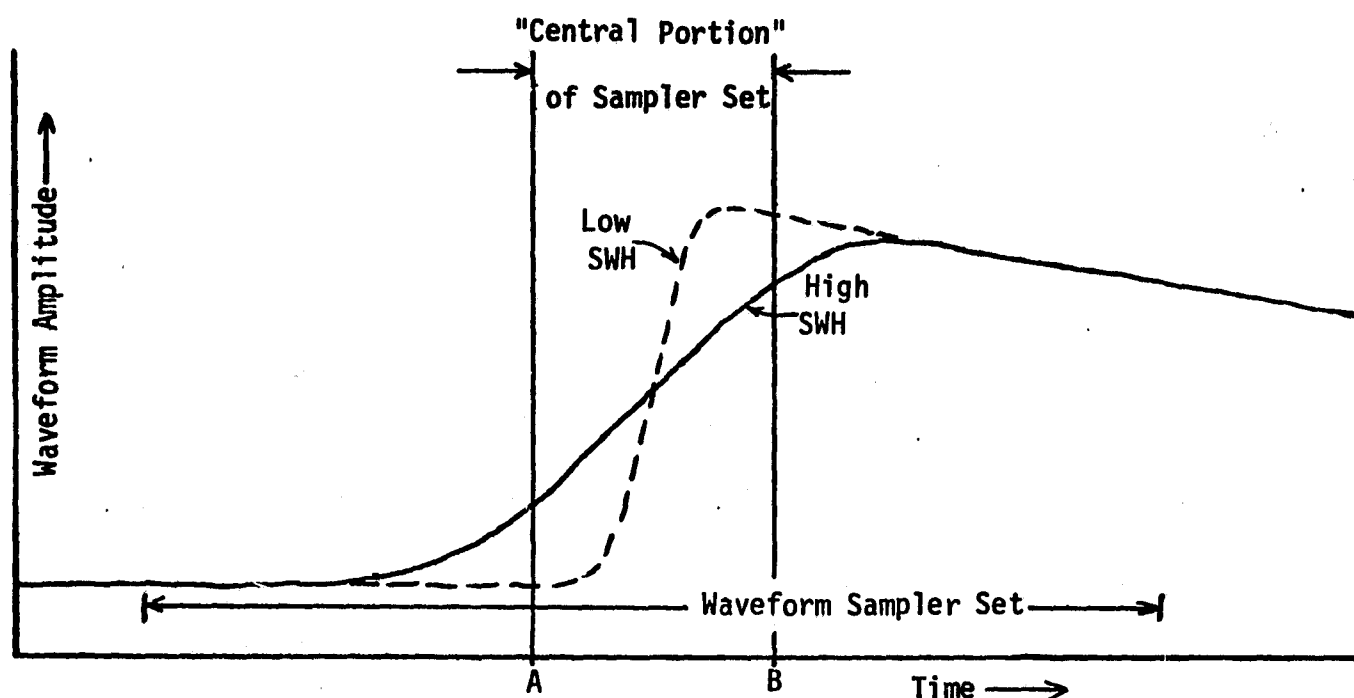
I.   GAIN CORRECTIONS OUTSIDE CENTRAL PORTION OF SAMPLER SET

   a.   Select Low SWH cases only from data set
   b.   For known attitude, fit waveform function
   c.   Use residuals outside region A-B as multiplicative gain corrections

II.   GAIN CORRECTIONS IN CENTRAL PORTION OF SAMPLER SET

   a.   Select High SWH cases only from data set
   b.   For known attitude, fit waveform function
   c.   Use residuals inside region A-B as multiplicative gain corrections

III.   (OPTIONAL) FINAL ADJUSTMENT OVER ENTIRE SAMPLER SET

   a.   For known attitude, fit waveform function
   b.   Use residuals over all samplers as final multiplicative corrections

Figure 14a shows the starting-point sampler gains from an average of Cali-
bration Mode II data, and Figure 14b shows the final set of gains after a pro-
cedure similar to that outlined in Figure 13. Notice the large (and, to this
date, unexplained) changes in the gains particularly in the later plateau por-
tion. For discussion later in the section on a plateau-region attitude estima-
tor, notice the (negative) non-zero slope in the Figure 14a smoothed sampler
gain vs sampler number curve in the region of waveform samplers 39-56. The
corresponding slope in Figure 14b is zero or slightly positive. Notice also
that the final gain set tends to be smoother gate-to-gate than the starting-
point set. The two sets of gains in Figure 14 are so different that we might
almost as well have started by assigning unit gains to all samplers as the
starting point for carrying out the gain fine-tuning. In other words, the
Calibration Mode II data are almost useless to us.

ATTITUDE ANGLE EFFECTS

When we applied the final sampler gain set described above to a variety of
experimental data in the work in early summer 1979, we found a number of regions
of over-ocean SEASAT-1 data in which the waveform fit results were poor because
the sampled plateau region decayed faster than allowed even at 0° off-nadir
angle (recall that the fastest decay is at 0° as shown in Figure 4). The six-
parameter waveform fitting process could not reach reliable estimates of the
other parameters because of the difficulties in the fitted off-nadir angle in
this situation. We were also finding that the off-nadir angle versus time
results, even in regions where the fit was not trying to produce negative
absolute values, did not correlate well with the attitude versus time results
from the attitude control system's attitude estimates. These various observa-
tions cast considerable doubt on our ability to use the attitude control system's

28

Figure 14a. Initial Sampler Gains from Calibration Mode II
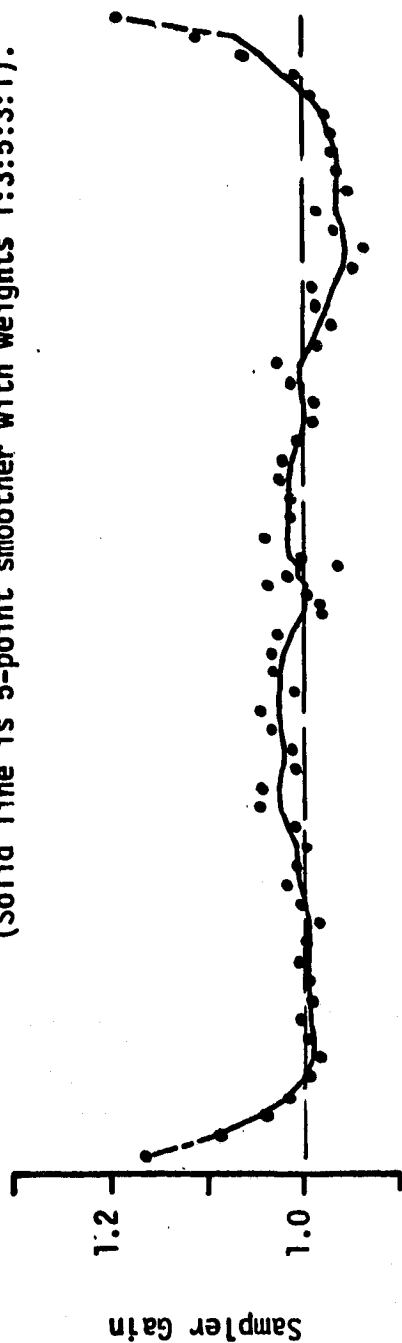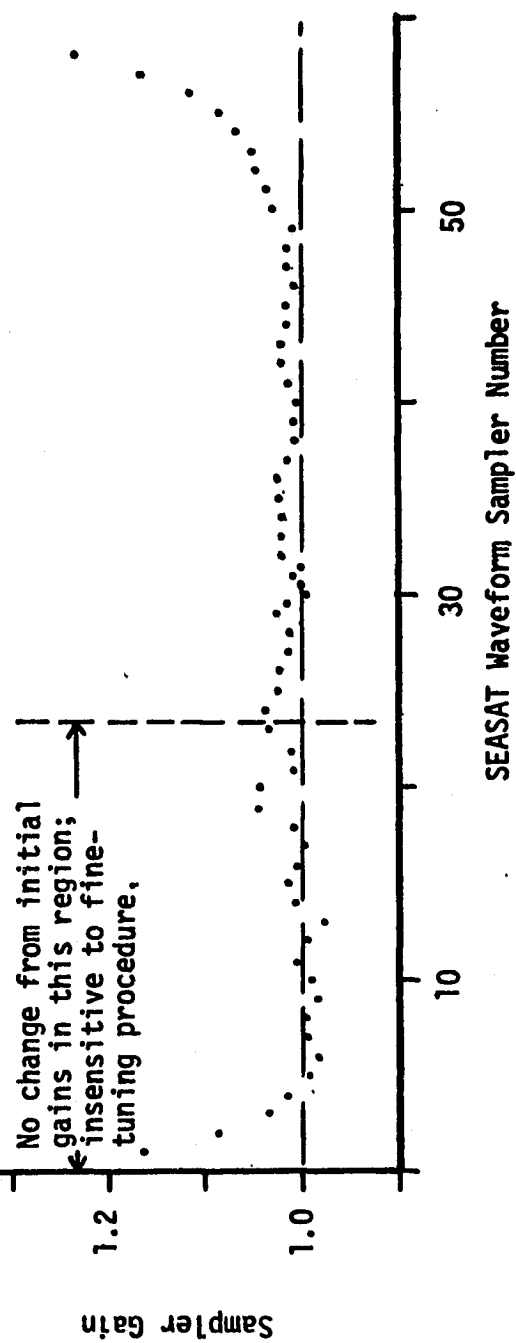(Solid line is 5-point smoother with weights 1:3:5:3:1).

Figure 14b. Final Sampler Gains After "Fine-Tuning."

No change from initial gains in this region; insensitive to fine-tuning procedure.

SEASAT Waveform Sampler Number

Sampler Gain

Sampler Gain

attitude estimates for input to the gain fine-tuning procedure. Figures 17-19, in the following report section describing a possible plateau-region attitude estimator, show our recent results supporting our claims of attitude estimation difficulties. We emphasize here that we need reliable attitude estimates only for the initial process of fine-tuning the individual waveform sampler gains. Once these on-orbit operate-status gains are determined, we assume that they are time-stable and we no longer require attitude estimates because the attitude can be one of the parameters fitted in the rest of the waveform processing.

Figure 15 is a schematic diagram to accompany this paragraph's discussion of interaction of the gain uncertainties and the attitude uncertainties. Suppose for example that only sample points at times earlier than B (Region I only in Figure 15) are fitted by a several-parameter waveform and that the SEASAT-1 attitude control system-estimated attitude ξ_S is used as a fixed, known attitude value. Some sort of gain adjustment over all waveform samples will then, in effect, force the plateau region (Regions II and III in Figure) waveform samples to lie on the curve labeled ξ_S in this figure. Suppose however that the _true_ attitude value were ξ_T instead, where $\xi_T > \xi_S$. In this case the plateau-region final gains would all be in error in such a way that when the attitude angle is treated as a fitting parameter the fitted attitude values would all be _lower_ than the true attitude values. In data spans where the true attitude itself is near zero, the waveform fitting procedure would then try to attain the impossible case of a negative absolute attitude value, and all other fit parameters would then be in error also. The situation just described is what we think did happen in the work in the early summer of 1979.

Figure 15. Figure for Discussion of Gain Biases and
            Pointing Angle Relationship.
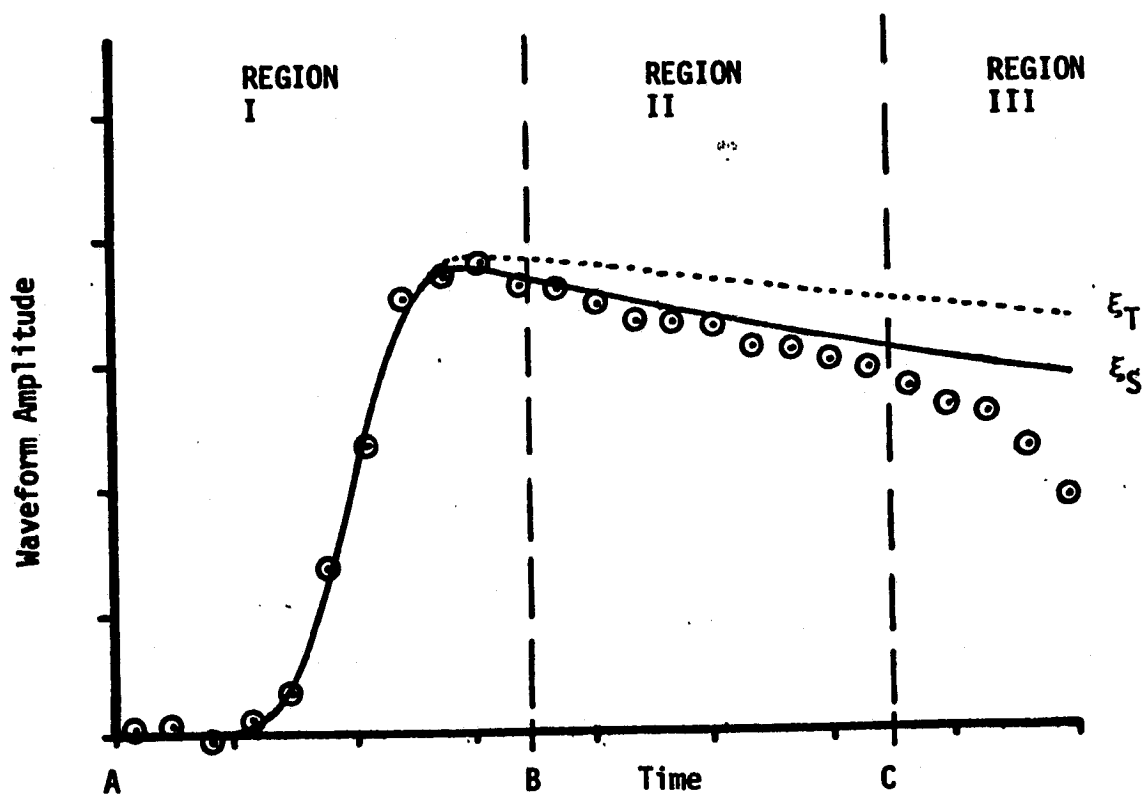
PLATEAU-REGION ATTITUDE ESTIMATOR

We are in the difficult position of believing that a sampler gain adjustment procedure is required and yet not having a reliable enough attitude knowledge to carry out the gain adjustment procedure. Once the gains are adjusted, our own waveform fitting can then vary the attitude as one of the fitted parameters but not before this adjustment has been completed.

The SEASAT-1 altimeter had a wide sampling gate later on the waveform plateau. This attitude gate, in a waveform region sensitive to attitude angle, was intended to provide data for attitude estimation. There was a similar attitude gate on GEOS-3 (sometimes referred to as the "attitude/specular gate" in the GEOS-3 literature) and these gate's locations are indicated on Figure 1. Unfortunately the SEASAT-1 attitude gate's scale factors were incorrectly set and the resulting attitude gate data are always at or near saturation. The result is that the attitude gates output is insensitive to attitude changes and thus is not useful to us as an attitude estimator.

The following several paragraphs sketch a "quick and dirty" attitude estimator using plateau region waveform sampler data. The estimator has calibration difficulties of its own but it should provide us with at least a look at the attitude trend and to identify data expanses in which the attitude is relatively constant. These constant attitude regions will then be input data for a revised sampler gain setting procedure. The basic procedure is to fit an $\exp(-\delta t)$ functional form to plateau region waveform samplers, and to estimate the attitude from simulation generated curves of δ vs ξ.

Recall that, as shown in Figure 1, the flat-sea impulse response function for the nadir-pointing ($\xi = 0$) SEASAT-1 radar altimeter has an exponential decay form at times greater than zero. For non-zero ξ, the behavior is not a simple

exponential but can still be fitted in a local region by an exponential. We allow for a noise baseline and assume that for low to moderate SWH the Region II waveform in Figure 15 may be represented by

$$W(t) = A \exp(-\delta t) + b .$$

We form the variable Z by

$$Z = \ln W(t) - b ,$$

and we do a least-squares fit of data from waveform samplers 39 through 56 to determine δ from

$$Z = \ln A - \delta t .$$

The b is estimated from the average of samplers 4 through 13, and we usually use a data smoothing interval of 10 seconds for each δ estimated.

For low to moderate SWH, the region of samplers 39-56 is well away from where the point-target response shape details affect the shape of the mean waveform, so there is no real difficulty caused by using the Ref. 9 expressions as a complete waveform description for this plateau region. In a separate simulation program we have generated an expected return waveform and then fitted the above exponential function to generate the curves of δ vs ξ given in Figure 16.

The δ estimated from experimental data will depend on what sampler gains are used for the samplers 39-56. We used the five-point-smoothed gains from Figure 14a. From the calculated $P_{FS}(t)$ at nadir point ($\xi = 0$) as in Figure 1, we know that the theoretical maximum value for δ is $\delta_m = 2.66 \times 10^{-3}$ ns^{-1}.

Figure 16. Attitude-estimating function vs attitude angle as function of SWH.
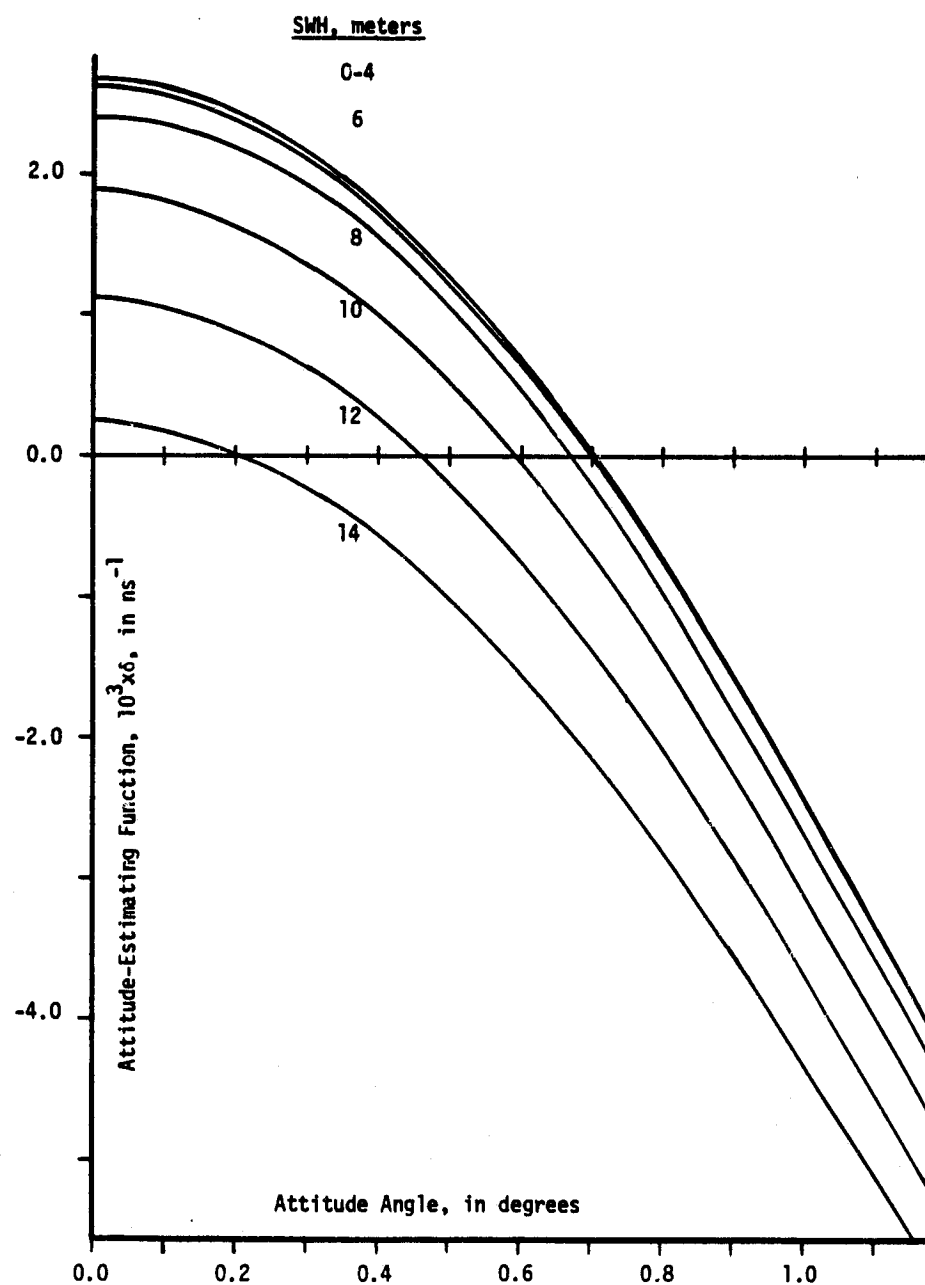
There were many regions of over-ocean SEASAT-1 data for which the experimental δ values were greater than δ_m, and we believe this was due to the operate-only gain trend (that is, to the different trend in the sampler gain vs sampler number in samplers 39-56 for Figure 14b as compared to Figure 14a). The first-order effect of a built-in erroneous gain vs sampler number trend would be a shift in the resulting fitted δ values. The various data we have looked through indicate that the maximum experimental δ values are probably around 3.6×10^{-3} ns^{-1}, so we subtract 0.94×10^{-3} ns^{-1} from all experimental δ before entering the curves of Figure 16 with δ and SWH to get an estimate of ξ. The first-order result of this 0.94 subtraction is a shift in the estimated ξ values.

Figures 17-19 show smoothed δ-estimated attitudes together with the attitude derived from the attitude control system. Figure 17 shows the two attitudes in fairly reasonable agreement in the first half of the interval shown, but with local maximum in different locations in the second part of the plotted interval. Figure 18 shows a different pass with more disagreement in locations of local maxima and minima. In neither Figure 17 nor Figure 18 is there strong indication of a bias or offset between the two different attitude estimates; such an offset would be the first effect of an error in the subtractive δ correction. Figure 19 however does show such a relative shift or offset; and the differences shown on Figure 19, particularly around 345 minutes, are significant to our waveform processing.

In summary, the saturation of the SEASAT-1 attitude gate prevents its use for attitude estimation. We have described the way in which an attitude estimator can be developed using plateau region sampler values (plus low-numbered samplers to estimate the baseline). This attitude estimator is not absolutely calibrated because of sampler gain problems, but should nonetheless be useful for attitude trend measurements.

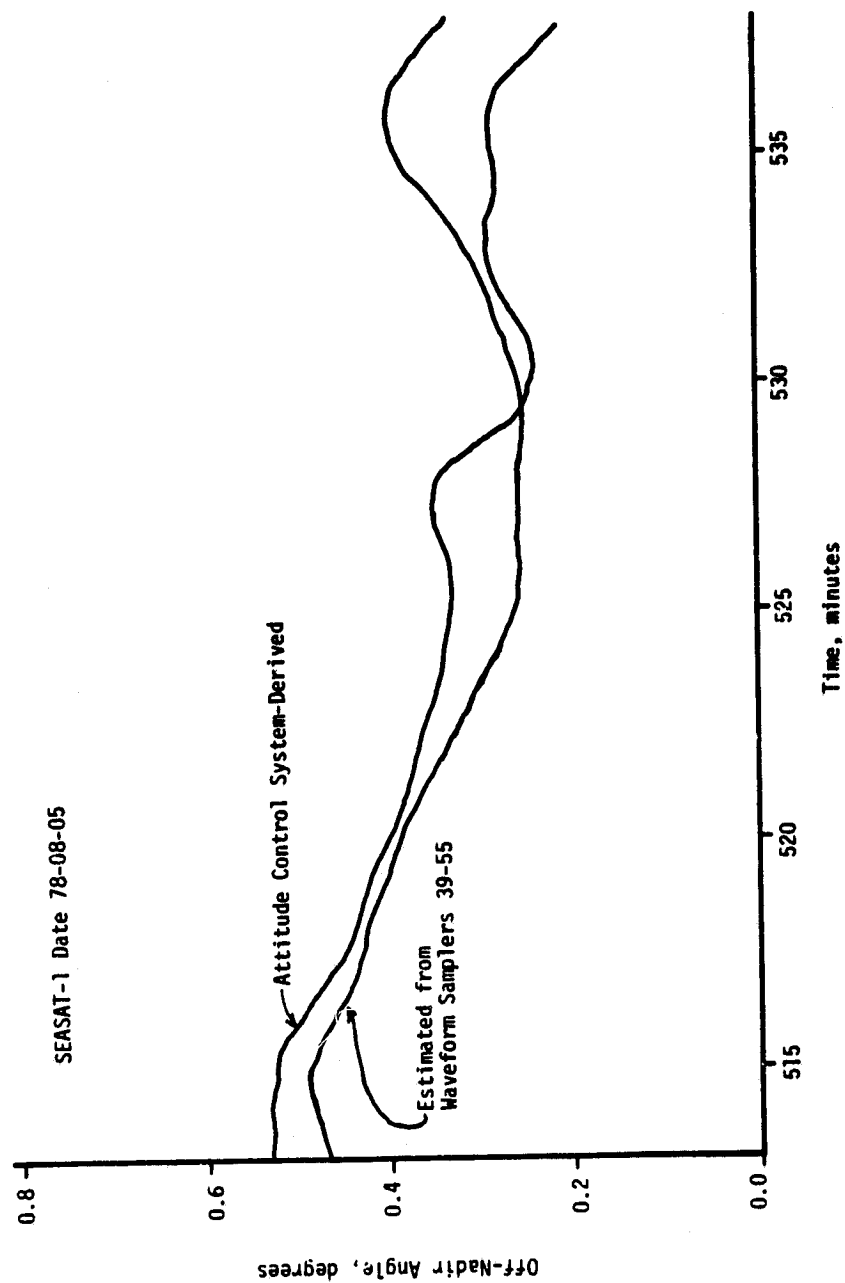Figure 17. SEASAT-1 estimates of off-nadir angle vs time.

36

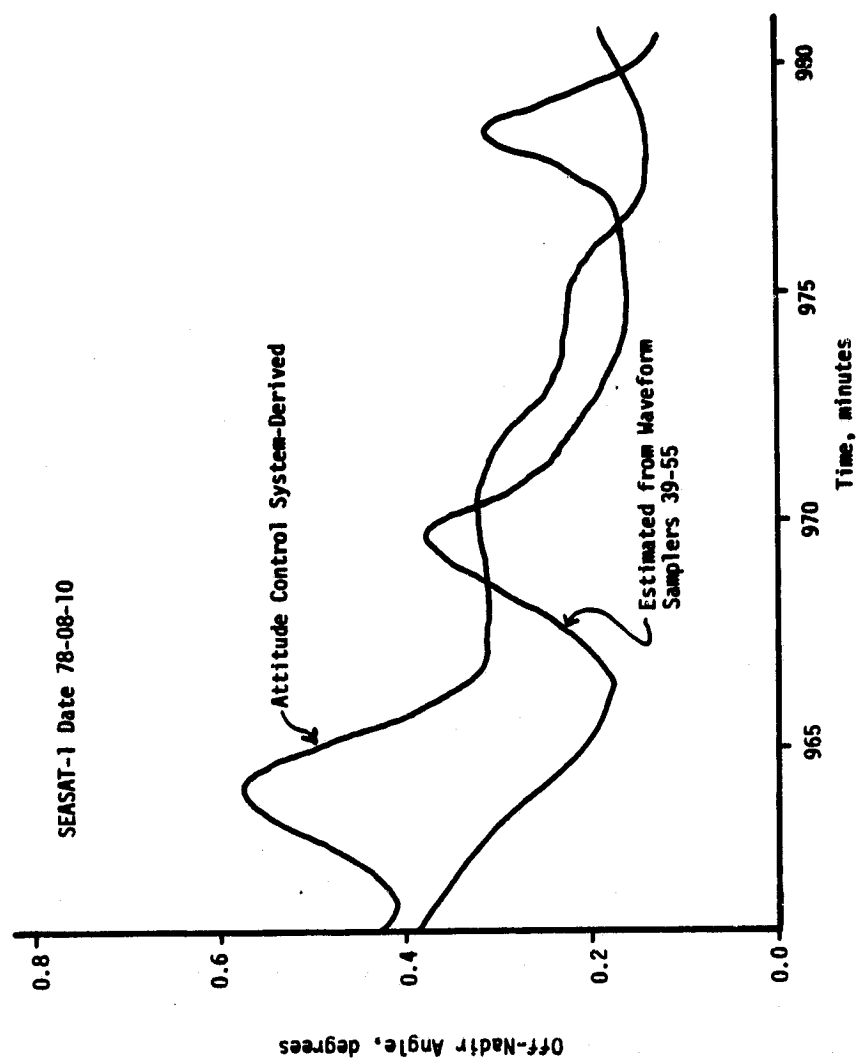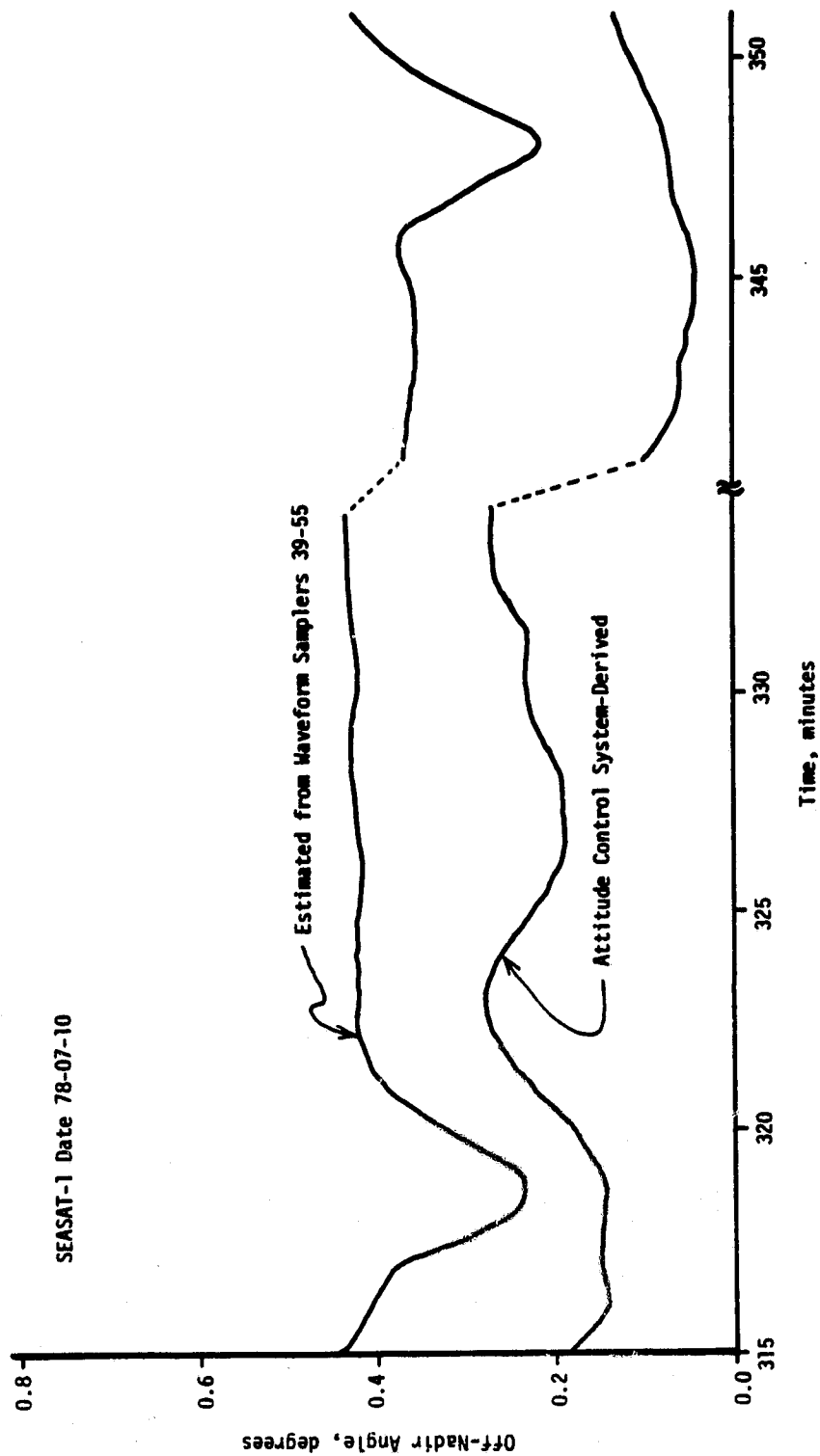Figure 18. SEASAT-1 estimates of off-nadir angle vs time.

Figure 19. SEASAT-1 estimates of off-nadir angle vs time.

SUMMARY

Our work has been directed toward fitting all 63 SEASAT sampling gate
values to a six-parameter model waveform function, once a process of adjusting
the individual sampler gains has been carried out. Ideally, this gain "fine-
tuning" would not be necessary; practically, we think it is very important for
the SEASAT situation. The model waveform for a nearly-Gaussian system point
target response has been described elsewhere (Ref. 9) together with a fuller
discussion of the background and assumptions for the radar altimeter mean return
waveform calculations. As shown by Figure 6 the SEASAT system point target
response is not describable as nearly-Gaussian, and the actual sampled point-
target response must be convolved with the general functional form from Ref. 9
(representing "everything else," everything except the point-target response) to
obtain the complete model waveform to be fitted to the 63 SEASAT waveform
samples. The waveform fitting procedure itself is completely straightforward;
it was sketched in Ref. 7 for a four-parameter situation and the extension to
six parameters is trivial. Our Fortran source program for the waveform fitting
contains a variety of minor adjustments which specifically adapt a once-general
fitting program to the special requirements of the SEASAT case, but these
changes are generally indicated by comments in our source listing (available now
on request, and to be published soon as a separate report).

The considerable difficulties which we have encountered have been in three
general areas; i) obtaining at final individual waveform sampler gains and
understanding why those gains differ from initial values from Calibration
Mode II, ii) incorporating the actual system point-target response into the
waveform model (and the knowledge of the point-target response also depends on
resolving sampler gain questions) and iii) obtaining reliable values for the

off-nadir attitude angle, at least for the initial sampler gain-adjusting phase of the work. Once sampler questions are resolved, incorporating the detailed system point-target response function into the waveform description is simple enough with the main difficulty being the practical one of markedly increased computation time resulting from a numerical convolution step within the fitting procedure. The question of individual waveform sampler biases remaining after using the best available calibration data is not unique to SEASAT; we had a similar situation in previous GEOS-3 work (where the waveform sampler biases were taken as additive rather than multiplicative) and, earlier, in work with the Skylab S-193 radar altimeter. Clearly if there were no difficulties indicated with the sampler individual gains and consequently no "fine-tuning" procedure necessary, then we would not require that the off-nadir attitude angle be known because this could be found as one of the fitted waveform parameters.

We would hope that our SEASAT-1 work to date would underscore the importance of good design of a relatively clean transmitted pulse with very dense sampling of the shape of the system point-target response, and would emphasize the need for great care in the design of the on-orbit calibration steps. The loss of useful SEASAT-1 attitude gate data points to one specific area for improvement in future systems. We have had difficulty using the on-orbit calibration data to interpret altimeter's waveform data while tracking (notably in the relative waveform sampler gains of Calibration Mode II vs the apparent gain fall-off in the late plateau samplers). Additional flexibility in the tracking operation, such as the ability to change the tracking point within the waveform sampler set, could be very useful for future radar altimeters.

REFERENCES

1. J. L. MacArthur, "SEASAT-A Radar Altimeter Design Description," SDO-5232, Applied Physics Laboratory, Laurel, MD, November 1978.

2. W. F. Townsend, "An Initial Assessment of the Performance Achieved by the SEASAT-1 Radar Altimeter," NASA TM-73279, NASA Wallops Flight Center, Wallops Island, VA, February 1980.

3. _____, "SEASAT Gulf of Alaska Workshop II Report," NASA 622-107, Jet Propulsion Laboratory, Pasadena, CA, January 1980; see report's Section 5.

4. N. E. Huang and S. R. Long, "A Study of the Surface Elevation Probability Distribution Function and Statistics of Wind Generated Waves," J. Fluid Mechanics (to be published).

5. E. J. Walsh, "Extraction of Ocean Waveheight and Dominant Wavelength from GEOS-3 Altimeter Data," J. Geophys. Res., Vol. 84, No. B8, pp. 4003-4010, July 1979.

6. P. G. Black and J. C. Wilkerson, eds., "SEASAT Storms Workshop Planning Document," Jet Propulsion Laboratory, Pasadena, CA, August 1979.

7. G. S. Hayne, "Initial Development of a Method of Significant Waveheight Estimation for GEOS-3," NASA CR-141425, Applied Science Associates, Apex, NC, August 1977.

8. G. S. Brown, "The Average Impulse Response of a Rough Surface and Its Applications," IEEE Trans. Antennas Propagat., Vol. AP-25, No. 1, pp. 67-79, January 1977; same paper also in IEEE J. Oceanic Eng., Vol. OE-2, No. 1, pp. 67-74, January 1977.

9. G. S. Hayne, "Radar Altimeter Mean Return Waveforms From Near-Normal-Incidence Ocean Surface Scattering," NASA CR-156864, Applied Science Associates, Apex, NC, April 1980.

10. G. S. Hayne, paper of Reference 9 above with minor revisions, IEEE Trans. Antennas Propagat. (to be published).